Blind Search of Faint Moving Objects in 3D Data Sets

Phan Dao*, Peter Crabtree and Patrick McNicholl

AFRL/RVBYC

Tamar Payne

Applied Optimization

Targets that move in the image of 2-D framing sensors are detected with less sensitivity than stationary ones. The reduction in sensitivity occurs when the object streaks during a frame's exposure time. Detection schemes that utilize photon uncorrupted coordinates (on imager) and arrival times can potentially outperform those that pixelate photon coordinates and bin arrival times by frame. Photon counting imager (PCI) technology, e.g. Los Alamos National Laboratory's Remote Ultra Low Light Imager, offers large format imaging sensors with sub-nanosecond time resolution, and hence provides a unique opportunity to enhance sensitivity with respect to the detection of moving objects. The ability to time tag and locate each photon results in a clear advantage in detecting moving objects; that can be attributed to the much reduced number density on a 3-D streak in comparison to its 2-D projection. In spite of a promise of higher detection sensitivity since the concept was introduced and proposed in 1993, to our best knowledge, no automated algorithm has been implemented to demonstrate the predicted gain in sensitivity. We demonstrate the anticipated sensitivity enhancement using a simulated object signature superimposed on measured background, and show that the limiting magnitude can be improved by up to 6 visual magnitudes. A quasi blind search algorithm that identifies the streak of photons, assuming no prior knowledge of orbital information, will be discussed and results shown. Performance of PCI sensors for this application will be presented for several telescope/imager configurations.

*3550 Aberdeen Ave, SE, AFRL/RVBYC

Kirtland AFB, NM 87117

Phan.dao@kirtland.af.mil

Report Documentation Page

Form Approved
OMB No. 0704-0188

1. REPORT DATE	2. REPORT TYPE	3. DATES COVERED
SEP 2013		**00-00-2013 to 00-00-2013**

4. TITLE AND SUBTITLE	5a. CONTRACT NUMBER
Blind Search of Faint Moving Objects in 3D Data Sets	5b. GRANT NUMBER
	5c. PROGRAM ELEMENT NUMBER
6. AUTHOR(S)	5d. PROJECT NUMBER
	5e. TASK NUMBER
	5f. WORK UNIT NUMBER
7. PERFORMING ORGANIZATION NAME(S) AND ADDRESS(ES) **Air Force Research Laboratory (AFRL),AFRL/RVBYC,3550 Aberdeen Ave, SE,Kirtland AFB,NM,87117**	8. PERFORMING ORGANIZATION REPORT NUMBER
9. SPONSORING/MONITORING AGENCY NAME(S) AND ADDRESS(ES)	10. SPONSOR/MONITOR'S ACRONYM(S)
	11. SPONSOR/MONITOR'S REPORT NUMBER(S)

12. DISTRIBUTION/AVAILABILITY STATEMENT
Approved for public release; distribution unlimited

13. SUPPLEMENTARY NOTES
2013 AMOS (Advanced Maui Optical and Space Surveillance) Technical Conference, 10-13 Sep, Maui, HI.

14. ABSTRACT

15. SUBJECT TERMS

16. SECURITY CLASSIFICATION OF:			17. LIMITATION OF ABSTRACT	18. NUMBER OF PAGES	19a. NAME OF RESPONSIBLE PERSON
a. REPORT **unclassified**	b. ABSTRACT **unclassified**	c. THIS PAGE **unclassified**	**Same as Report (SAR)**	**12**	

1. INTRODUCTION

Traditional imagers such as a charge-coupled-device (CCD) quantize the position and arrival time of each signal photon. Arrival time information cannot be finer than the frame exposure and read-out time. The image of a moving target is bound to produce a streak which is superimposed on the background. The registration of signal photons in more than one pixel results in a reduction of the signal to noise ratio and detection sensitivity. In contrast, a photon counting imager (PCI) records the position and time of each photon event. If the target's angular velocity is known, each photon can be transformed into a moving coordinate frame and all the signal photons can be mapped into a single pixel. The mapping would preserve the maximum SNR. The purpose of this study is to demonstrate an algorithm for searching the angular velocity of an observed object and detecting the latter without *a priori* information. Detection is therefore achieved with improved sensitivity when compared to detection in 2D data sets. For a moving object, the minimum detectable object's size, based on thresholding pixel values, scales as the square root of angular velocity for CCD-like imagers because the SNR scales as $N_{object}/\sqrt{N_{bgd}}$. In contrast, a photon-counting detector has a threshold that is independent of velocity. The signal however scales with the time the object stays in the field of view. Cheng Ho was the first to propose the use of a PCI for detecting dim moving space debris [Ho 1993]. With such a device, the data is collected in a 3-dimensional (3D) format, i.e. a list of positional x and y and time t for all photons. This increase of dimensionality greatly enhances the statistical significance of the moving object's linear streak. When the number of photons on a streak exceeds ~10, one has overwhelming evidence that they are not due to background. Such a streak corresponds to a detection limit orders of magnitude lower than what can be achieved with a CCD-like device. [Ho 1993] proposed an algorithm based on hierarchical line searching and applied it to simulation data sets. [Priedhorsky 2005] proposed an advanced search algorithm based on 3-D Fast Fourier transform and applied it to the x-y-t list. With this technique, the authors can create any projection of the data cube by performing an inverse FFT of a 2-D slice of the Fourier domain cube that is perpendicular to the desired velocity. The detection is based on searching all possible projections for the pixel that exceeds detection threshold. The use of FFT would speed the construction of the projection because it scales as $(N\ log\ N)^2$ instead of N^3 as achievable with a naïve approach of computing 2-D projections [Thompson 2013]. The authors have not reported results on the implementation of the proposed technique. To our best knowledge, this study is the first demonstration of the detection of moving objects in a background measured with a PCI.

2. EXPERIMENTAL SET-UP

The Magdalena Ridge Observatory (MRO) fast-tracking 2.4 m telescope (see Fig. 1a) is a relatively new high-technology facility located at 10,612 feet atop the Magdalena Mountains in central New Mexico [33° 59' 6.0" N, 107° 11' 21.0" W], and is part of the New Mexico Institute for Mining and Technology - a small research and engineering university located in Socorro, NM. The MRO 2.4 m is one of the largest telescopes in the world whose primary mission is the physical characterization of small bodies (both natural and artificial) within the Solar System. The observatory is intended for both astronomical research and resident space object (RSO) characterization. The 2.4-meter control system is designed to provide convenient and accurate

non-sidereal tracking, and the telescope is capable of rapid movement with slew rates up to 15°/sec. The telescope can accommodate a wide variety of instrument systems, and supports the fabrication, integration, and operation of new instrumentation as well as the development of new and innovative observational techniques.

The 2.4 m telescope is a modified Ritchey-Chrétien design, with an overall focal ratio of f/8.9 and an unvignetted field-of-view (FOV) of 15 arc-minutes. The 12-inch acquisition telescope mounted on the main telescope has a FOV of about 0.5 degrees. The intrinsic resolution of the optical system is defined by a full-width half-maximum (FWHM) of 0.2 arc-seconds for a point source. There are two Nasmyth ports (which can support larger and heavier instrumentation) and four bent Cassegrain ports, one of which permanently hosts a Shack-Hartmann wavefront sensor to facilitate automatic collimation and focusing. Therefore, the facility can simultaneously mount up to five instruments at any given time. Median good seeing at the site is 0.7 arc-seconds, and the faintness limit of the telescope for visual wavelengths is about 25th magnitude. Data was collected at the MRO with the photon counting imager (PCI) coupled to the 2.4 m telescope via Nasmyth port. A side-view of the Nasmyth port equipment rack housing the instrumentation is shown in Fig. 1b, and a nearly top-down view of the installed PCI sensor head and filter wheel is shown in Fig. 1c. The purpose of the measurement campaign was to collect unresolved signatures of RSOs and stellar objects. For the observations made using the PCI, both geostationary Earth orbit (GEO) and medium Earth orbit (MEO) objects were initially located by pointing the telescope along a track calculated from recent two-line elements (TLEs). During the most recent campaign, observations were made over 3 sessions spanning the period 4-6 Dec 2012. During that time we observed and collected data on both calibration stars and RSOs, mainly those residing in GEO. A major objective of this effort is to collect data supporting the exploration of various space surveillance applications able to leverage the very high temporal resolution and sensitivity of a PCI.

(a) (b) (c)

Figure 1. The photo in (a) shows the MRO 2.4m telescope facility. The photo in (b) shows a side view of the Nasmyth port equipment rack in which the PCI was installed. The installed PCI sensor head and filter wheel are shown in (c), with the optical path illustrated by red arrows.

The PCI system was procured from Sydor Instruments, and is a true photon counting imaging detector based on a 40 mm diameter low-noise S20 photocathode, multi-channel plate (MCP) stack, and cross delay line (XDL) readout. The PCI sensor head produces five signal outputs;

four outputs from the XDL readout (2 for each orthogonal wire wound anode), and one output measuring voltage across the MCP stack. The five channels are amplified and fed into a constant fraction discriminator (CFD) to estimate pulse arrival time (ideally) invariant to pulse height. The CFD outputs are then captured by a time-to-digital converter (TDC) installed in a rack-mounted PC running MS Windows 7. The PCI is extremely sensitive and fast, but exhibits a very limited dynamic range on the order of 1 MHz. To provide some additional control over dynamic range, the sensor head is coupled to a consumer-grade filter wheel (Orion Nautilus, 4x2") housing a light block and three ND filters with optical densities (ODs) of 0.7, 1.8, and 3.0. TDC data acquisition was accomplished using custom software developed in MS Visual C++ 2005; the main GUI is shown in Fig. 2. The output of the TDC is a string of 32 bit data words, each corresponding to either pulse arrival time information for one of the 5 channels or an error message. The inclusion of a rollover counter provides 48 bit resolution of the arrival times, and high resolution mode of the TDC provides a digital resolution of 25 picoseconds. An image can subsequently be reconstructed using at minimum the four XDL outputs; the arrival position of the charge cloud along a given axis is proportional to the difference in the time of arrivals of the pulses emitted from each end of the corresponding wire wound anode. The MCP signal is not required for image generation, but can be useful in terms of discriminating valid events.
The spatial resolution of the PCI is relatively poor, and was measured in the lab to be approximately 250 μm FWHM in both the x and y directions. The temporal resolution (jitter) was indirectly measured to be approximately 294 picoseconds standard deviation. The PCI dark count rate is roughly 4x10-2 photo-electrons/s/mm2.

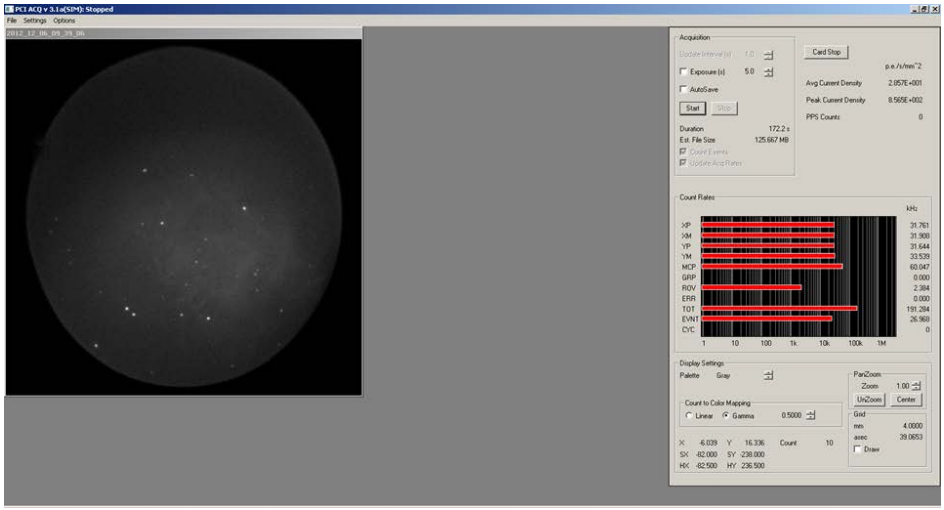

Figure 2. The top-level screen of the custom data acquisition software developed for the PCI sensor.

3. SEARCH TECHNIQUE

As mentioned, the statistical significance of a streak of as few as 10 photons is overwhelming in 3-D. In 2-D data sets, the expected number of photons on a streak, λ_{2D}, is approximated by (1).

$$\lambda_{2D} = \frac{B}{D^2} D \tag{1}$$

where B is the number of background photons in the data set and the number of resolution cells D is approximated as the ratio of the imager's width to the positional uncertainty $D \simeq d/\sigma$. In a data cube, the expected number of photons is approximated as follows.

$$\lambda_{3D} = \frac{B}{D^2 D'} D' \tag{2}$$

The temporal D' is approximately the same as D because the streak's volume where the signal photons are located is dominated by positional uncertainties. With time resolution less than 1 nanosecond and the object's transit time ~ 1 sec, the effect of time uncertainty can be neglected. Note that λ is also the variance of a Poisson distribution which we expect to be appropriate for the statistics of photons. For the Photek PCI, $\sigma \simeq d/400$ or D≃400. For such a distribution of background photons, the number of random photons on a streak (or tube) is 400 times smaller in 3-D, $\lambda_{3D} \simeq \lambda_{2D}/400$. The probability P of finding a tube with more than *m* photons in a data cube of N photons is estimated by (3) and also shown in Fig. 3.

$$P(m) = \left(e^{-\lambda} \sum_{k=0}^{m-1} \frac{\lambda^k}{k!} \right)^N \tag{3}$$

In Fig. 3, the leveling off of the probability *P(m)* for *m* equal to or higher than 8 is an artifact of calculating with double precision numbers. It is expected that the trend is linear and shown by the dashed line. Therefore, the probability of finding 10 or more photons on streak is less than 10^{-8}. The objective of the detection is simply to search for streaks with 10 or more photons. We are reassured that 10 photons is a conservative threshold for detection and finding 10 photons is achievable.

The technique we use for the search is based on the research conducted in the field of vision research and LADAR 3D analyses. Fischler published an iterative method to estimate parameters of a mathematical model from a set of observed 3-D data [Fischler 1981]. Based on the principles of Fischler's RANdom SAmple Consensus (RANSAC), we developed an algorithm called RANdom SAmple Consensus –Moving Target (RANSAC-MT) to search for data points that conform to a linear model and the constraints imposed by the PCI imager. As with RANSAC, RANSAC-MT is a non-deterministic algorithm in the sense that it produces a reasonable result only with a certain probability. This probability increases as more iterations are allowed. The relationship between the number of iterations T and the desired probability *p* of finding the streak is shown in (4).

$$T = \frac{\log(1-p)}{\log\left(1-\left(\frac{m}{B}\right)^2\right)} \tag{4}$$

Equation (4) dictates the tradeoff between speed and sensitivity. The pseudocodes of RANSAC-MT are shown in Fig. 4. The codes are implemented in MATLAB in this study. They are not meant to be an operational solution with useful speed. The codes are however suitable for efficient scaling because the random selection of pairs of points, found inside the *while* loop (Fig. 4), can be executed in parallel. The selection of the winning pair can be reconciled once the set of pairs is processed.

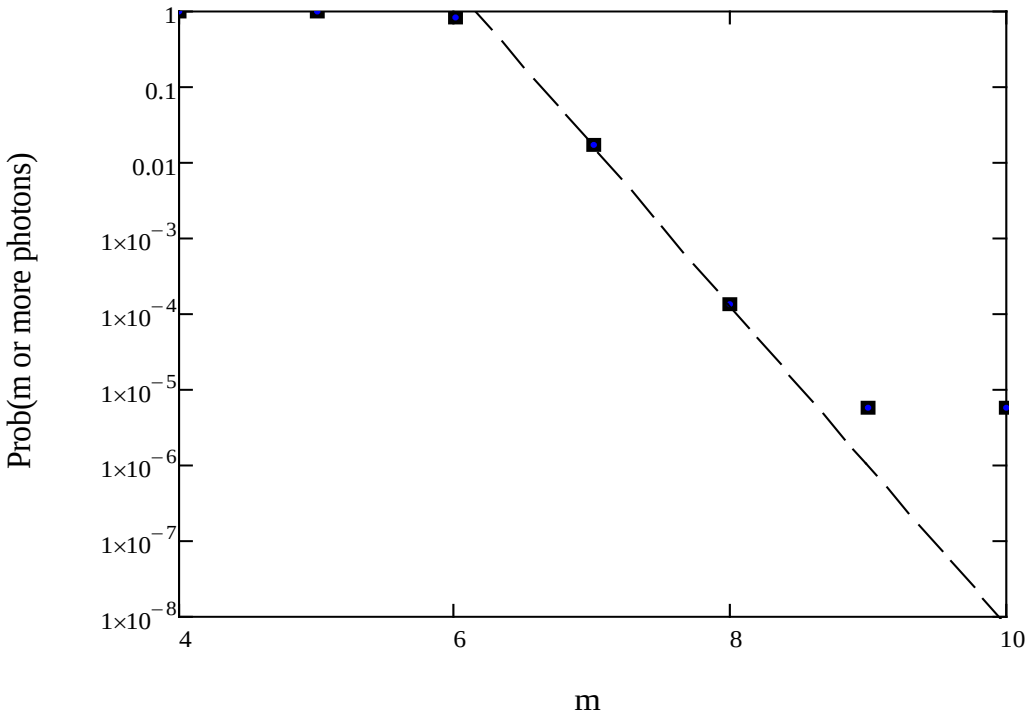

Figure 3. Occurrence probability of a streak with m or more background photons

```
Pseudocodes for RANSAC-MT algorithm

bestSupport = 0; bestStreak(3,1) = [0, 0, 0]
bestStd = infinity
 i = 0
ε  = 1 – forseeable_support/length(point_list)
N=round (log (1 – α )/log (1 –  (1 – ε ^3))
while (i <= N) AND (line not parallel to star
track)
 j = pick 2 points randomly among (point_list)
 line = pts2line(j)
 dist = dist2plan(line, point_list)
 s = find(abs(dist)<= threshold)
 std = Standard_deviation (s)
 if (length(s) > bestSupport or (length(s) = …
  bestSupport and std < bestStd)) then
  bestSupport = length (s)
  bestStreak = pl;
  bestStd = std;
 endif
i = i+1; endwhile
```

Figure 4. RANSAC-MT pseudocodes

4. RESULTS

The 3D data sets we analyzed consist of a data cube of actual x-y-T values collected with the telescope pointed at the calibration star field SA 98-1119. Object's signatures are simulated with different signal strength and added to the list. We varied the strength as well as angular velocities. The x-y-T values of the photons are simulated to have random arrival times and positional uncertainties consistent with the Photek PCI.

Before applying RANSAC-MT, to reduce false alarms due the star background, the star signatures are removed. This step can be easily taken because the motion or lack of motion as in the case of a sidereal scan is known. Furthermore, one can find and remove the stars in a data set with an arbitrarily long collection window for maximum sensitivity. An example of 3D data set, collected near SA 98-1119 (103.15 deg. right ascension and -0.241 deg. declination) but with all the stars removed, is shown in Figure 5.

Figure 6 shows the data cube with the background photons colored in red and the photons discovered by RANSAC-MT colored in blue. In this particular run, 40 simulated streak photons are added to the background photon list with appropriate x-y-t values. The background of 1.2E4 photons is consistent with that of a 6 inch telescope with F/40 optics operating against a 22th magnitude per arc-sec^2 sky. The Photek, being a first generation PCI, is limited in terms of maximum photon count (1E6/sec). The parameters we have selected correspond to a 6-inch telescope staring at a fixed right ascension and fixed declination and the moving object is in a 2000km orbit and near zenith track. We'd like to assess the sensitivity of such a system and compare it to that of a CCD sensor. More modern PCIs have maximum count rate 1 or 2 orders of magnitudes higher. The choice of the number of background photons is based on the desire to stay within the limitations of our PCI maximum count rate and assess our current sensor. The discovered signal photons are colored in blue for easy distinction. The positions of the signal photons are placed randomly but according to our

instrumentation's spatiotemporal uncertainties. In Figure 7, the photons are projected in a direction close to the retrieved velocity to show the improved SNR in the 2-D projection. That projection corresponds to a coordinate transformation that maps the object's photons to a single point.

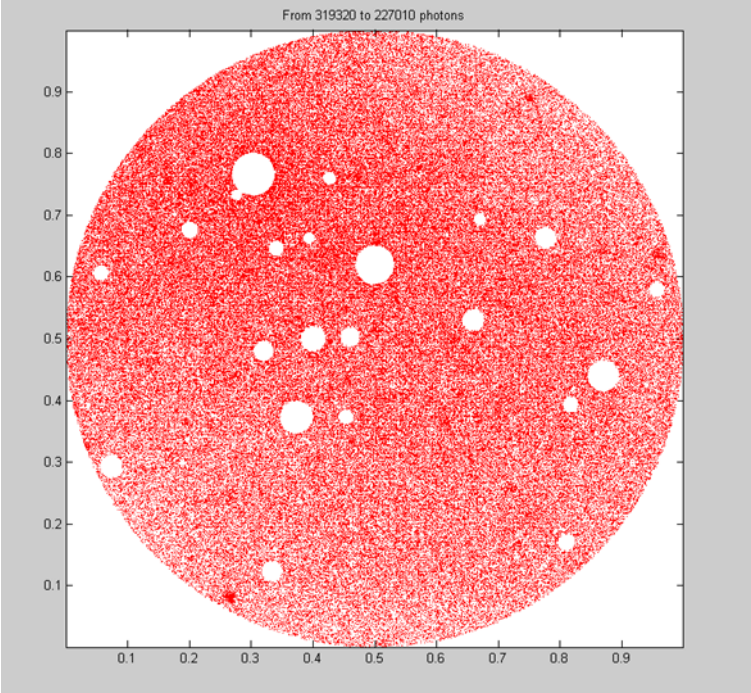

Figure 5. The stars have been removed from the data cube.

The trade off between sensitivity and recovery success rate is shown in Figure 8. RANSAC-MT is a non-deterministic algorithm and the probability of recovery improves with the number of draws.

5. DISCUSSIONS AND CONCLUSIONS

While RANSAC-MT did not achieve the sensitivity of detecting 10 photon streaks, as indicated by the statistical significance evaluation, it does detect streaks with 20 photons with a success rate of close to 50%. The improvement in sensitivity and its comparison to traditional CCDs is presented in Table 1. While CCDs have better a quantum efficiency, the performance of a 6 inch PCI-based telescope is 3.6 visual magnitudes better than a CCD-based system of same aperture. Because our Photek is a first generation device with limited photon count rate, the first benchmark has been based on a moderate aperture of 6 inch and shown in red in Table 1. With a realizable improvement in count rate (benchmark 2), later generation PCIs are projected to be able to handle a 14 inch telescope and the performance is as shown in green in the Table 1. We demonstrated that a 6 inch system can detect orbiting debris, 9 cm in diameter and with albedo of 0.2, at 2000 km altitude. With PCIs running at higher count rate and mounted on a 14 inch telescope, debris with diameter of 2 cm may be detected in similar circumstances. We recognize that RANSAC-MT may not be optimized for speed and the use of a larger aperture will exponentially increase retrieval time. Therefore, we may have to explore alternative search algorithms and particularly revisit the proposed idea of 3-D Fourier rendering [Priedhorsky 2005].

6. ACKNOWLEDGEMENTS

Support from the Space Object Surveillance Technology Program Manager, Dr. Jeremy Murray-Krezan, the Mission Lead, Dr. Lawrence “Robbie” Robertson, and the SSA community at the Space Vehicles Directorate is well appreciated.

References

[Ho 1993] C. Ho, W. C. Priedhorsky, and M. Baron, “Detecting small debris using a ground-based photon-counting detector,” in Space Debris Detection and Mitigation, A. F. Allahdadi, ed., Proc. SPIE 1951, 67–75 (1993).

[Priedhorsky 2005] William Priedhorsky and Jeffrey J. Bloch, *Optical detection of rapidly moving objects in space*, Applied Optics, Vol. 44, No. 3, 20 January 2005.

[Thompson 2013] Communications with Dr. David Thompson (Los Alamos National Laboratory).

[Fischler 1981] Martin A. Fischler and Robert C. Bolles,"Random Sample Consensus”, Comm. of the ACM 24 (6), June 1981.

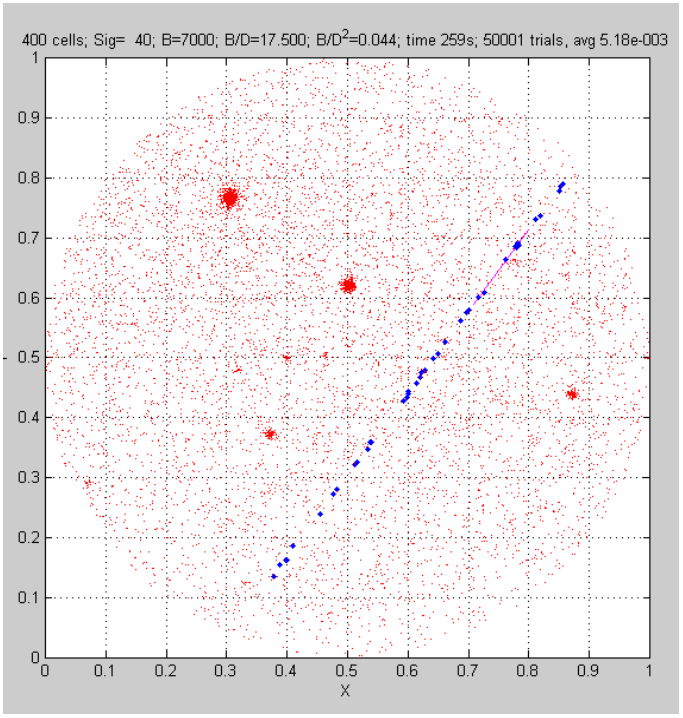

Figure 6. The object signal photons were retrieved by RANSAC-MT and marked as blue dots. In this example, the signal consists of 40 photons.

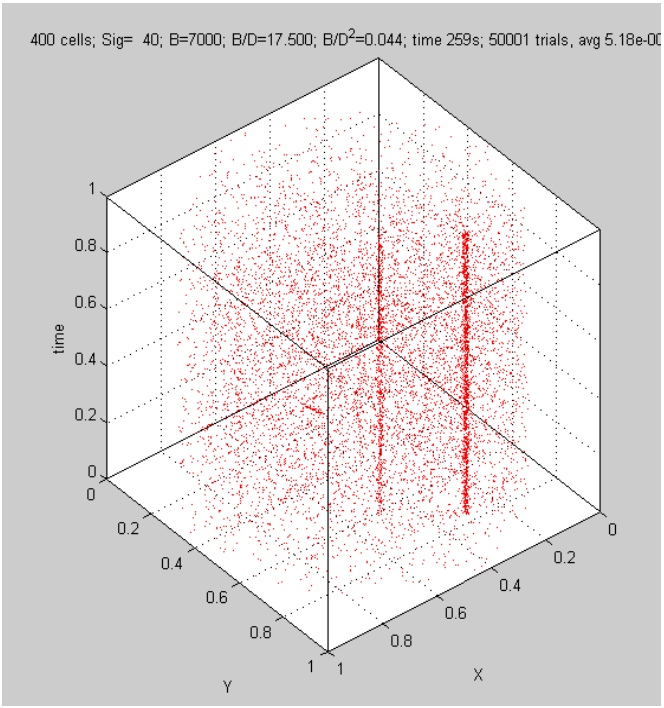

Figure 7. With the streak found and the velocity recovered, the data cube is reoriented to show the projection of the photon dots clearly show the clump of signal photons near the center. The star photons were reinserted to show the significance of the clutter.

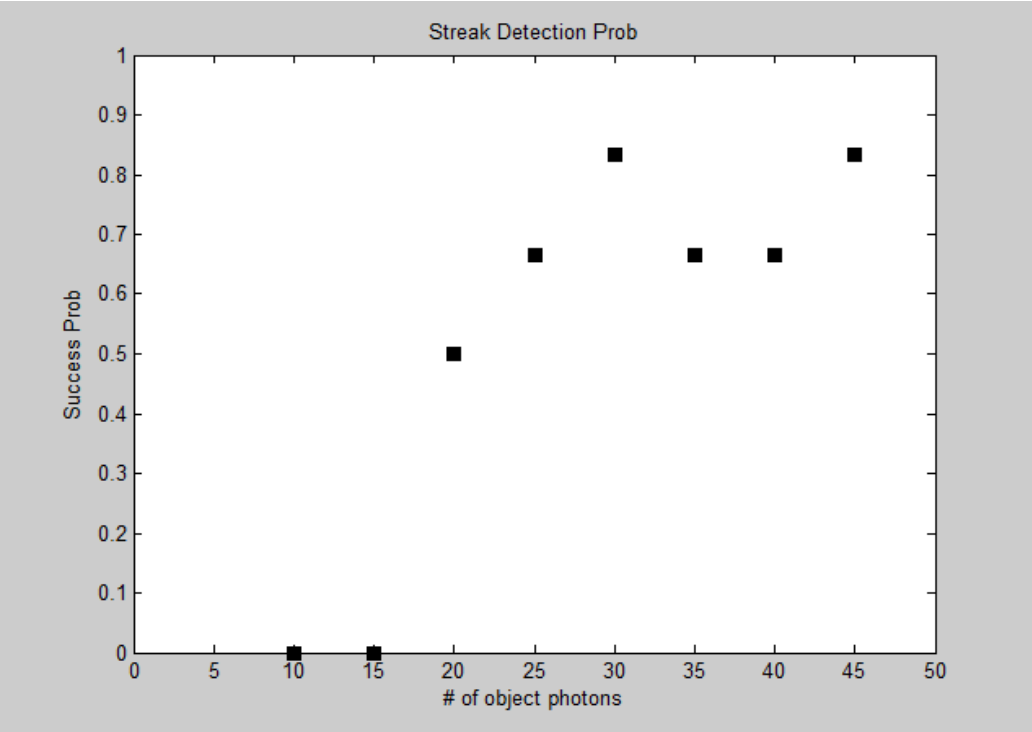

Figure 8. Probability of retrieval. A probability of 50% is achieved near 20 photons.

	Tel Dia	FPA Dimension	Focal Ratio	Background Mag	Integration Time	Bgd pe	RSO Mag	# of Photons	SNR
RAVEN stationary target	14 in	1Kx1K 13mm CCD	11	19	24 s		18		18[i]
RAVEN 0.36 deg/s mov target	14 in	1Kx1K 13mm CCD	11	22	0.7 s		12.4[ii]	6000 900 S20	18[i]
6in RAVEN mov target	6 in	1Kx1K 13mm CCD	40	22	1.0 s		11.1		20
6in RAVEN PCI mov trgt	6 in	400x400 20mm S-20	40	22	1.0 s	1.2E4	15.5 14.7	10 20[iv]	N/A
RAVEN-PCI moving target[iii]	14 in	400x400 40mm GaAs	11	22	0.7 s	4.4E5	18.1	10	N/A

i CCD benchmark for stationary RSOs according to Dr. Steve Gregory (Boeing)
ii Magnitude calculated to match the threshold SNR set by SG benchmark
iii RANSAC-MT has not been shown to handle 14 in/11 FR telescope background
iv 20 photon detection is achievable with current algorithm.

Table 1. Sensitivity of PCI sensor in comparison to CCD sensor.